Collision-induced fusion of two C_{60} fullerenes: Quantum chemical molecular dynamics simulations

Jacek Jakowski*
National Institute for Computational Sciences, JICS-ORNL, One Bethel Valley Road, Bldg 5100 ms 6173, Oak Ridge, Tennessee 37831, USA and Cherry L. Emerson Center for Scientific Computation and Department of Chemistry, Emory University, 1515 Dickey Drive, Atlanta, Georgia 30322, USA

Stephan Irle†
Institute for Advanced Research and Department of Chemistry, Nagoya University, Nagoya 464-8602, Japan

Keiji Morokuma‡
Cherry L. Emerson Center for Scientific Computation and Department of Chemistry, Emory University, 1515 Dickey Drive, Atlanta, Georgisa 30322, USA and Fukui Institute for Fundamental Chemistry, Kyoto University, Sakyo, Kyoto 6006-8103, Japan
(Received 27 April 2010; published 24 September 2010)

We characterize the collision-induced fusion reaction of buckminsterfullerenes by means of direct self-consistent-charge density-functional tight-binding molecular dynamics simulations. In agreement with experimental data, we find that the highest probability of fusion is for collisions with incident energy range of 120–140 eV. In this energy region, fusion occurs by way of the formation of hot, vibrationally excited peanut-shaped structures within 1 ps. These nanopeanuts further undergo relaxation to short carbon nanotubes and are cooling by evaporation of short carbon chains during the next 200 ps. The size of the fusion product after the evaporation agrees well with the average size of carbon clusters experimentally detected after collisions on the microsecond time scale. The average number of sp^3 carbons in our simulations is in an excellent correlation with experimental cross sections.

DOI: 10.1103/PhysRevB.82.125443 PACS number(s): 68.35.bp, 63.20.dk, 71.15.Pd, 73.22.−f

Fullerenes and carbon nanotubes (CNTs) are promising building blocks of nanotechnology for the production of nanoscale devices and nanomachines with complex geometry. They are chemically very stable and inert. This suggests that the nanomachines, once synthesized from such nanoblocks, should remain structurally stable. Unfortunately, the required technology to allow engineered production of machines and devices at nanoscale level is still in its infancy. The controlled growth of specific fullerene isomers and CNTs, and furthermore the controlled assembly of smaller carbon nanoblocks into larger units remains a major challenge in nanotechnology for material science and CNT research.[1,2] Potential applications include molecular machinery, sensors, catalysts, polymer composites, biological and medical materials, molecular data storage, and single-gate electron transistors.

As noted by Zhao *et al.*, fusion of smaller components into a larger whole is a ubiquitous process in condensed matter. At the molecular level, it corresponds to chemical synthesis.[3–6] At the pioneering age of fullerene science, the merging of two spherical units to form a larger structure seemed impossible, due to very high energy required to break a multitude of carbon cage bonds.[4] First coalescence experiments were performed by Whetten[6] and Campbell.[7,8] Whetten *et al.* have reported mass spectroscopy (MS) measurements of hot, dense C_{60} vapors, revealing their coalescence to higher fullerene adducts with MS maxima around multiples of the initial mass minus one or two C_2 units.[6] Campbell presented evidence for coalescence of fullerenes via high-energy collision[5,7,8] under well-defined single-collision conditions. The processes described by Campbell[5] focus on collisions at hyperthermal energies and include collision-induced fragmentation and ionization, charge transfer and endohedral fullerene formation. In addition, scattering, fusion and (multi) fragmentation in fullerene-fullerene collisions have been discussed by the same authors. A systematic description of fullerene reaction dynamics results can be found elsewhere.[4,5]

In addition to studies of reactive C_{60} collisions, fusion of more complex carbon nanostructures has been reported in the literature.[4,5,9–12] Yoon *et al.* reported unusually fast fusion of two CNTs originating in a single Y junction, proposing a zipper mechanism for this coalescence based on series of orchestrated Stone-Wales transformations.[10] Jin *et al.* presented a technique for fusion of CNTs via controlled head-to-head and head-to-side "plumbing" engineering for nanotechnology applications.[11] However, no molecular dynamics (MD) simulations of nanocarbon fusion processes based on a quantum chemical potential have been reported.

Here we report our theoretical efforts related to collision-induced fusions of C_{60} fullerenes, aimed at improving understanding of processes related to assembling of smaller carbon nanoblocks into larger units. This reaction can be considered as a prototype reaction for the fabrication of short CNTs and other, more complex structures.

We modeled fusion of two C_{60} fullerene cages by means of direct MD simulations, where the electronic structure (both cold and thermally excited) was computed on the fly within the framework of the self-consistent-charge density-functional tight-binding (SCC-DFTB) theory.[13–17] Overall we performed around 1000 Born-Oppenheimer MD simulations of collision by applying various initial conditions. Em-

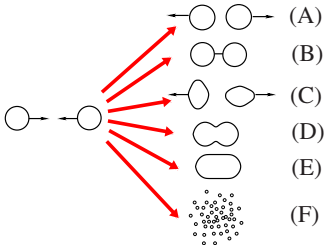

FIG. 1. (Color online) Schematic outcomes of collision between fullerenelike (denoted as circle or oval) structures: (a) nonreactive elastic scattering, (b) dimerization/polymerization, (c) collision-induced internal reorganization/inelastic scattering, (d) partial coalescence, (e) full coalescence, (f) fragmentation. Black arrows on panels (a) and (c) and on left panel represent velocity vector of corresponding unit.

ploying direct MD techniques with explicit quantum-mechanical treatment of electronic structure allows to address such questions as: (a) what is the nature of fusion reaction between carbon nanoparticles, (b) how does the outcome of the collision depends on the incident velocity, (c) what is the role of electronic excitations (via electronic temperature) in the fusion reaction, (d) what is the effect of long time, post collision relaxation of fusion products, (e) what is the prospect for controlled fusion of carbon nanostructures and its application in nanoscale engineering, and (f) how reliable are SCC-DFTB/MD simulations for the description of high energy fusion reaction in comparison to experiment.

I. OVERVIEW OF COLLISION ROUTES

The outcome of collisions between fullerenic structures can be classified as one of the following routes: (A) nonreactive scattering/elastic collision ($A+B \rightarrow A+B$), (B) dimerization ($A+B \rightarrow A-B$), (C) nonreactive reorganization/inelastic scattering ($A+B \rightarrow A^*+B$ or $A+B \rightarrow A^*+B^*$), (D) partial coalescence ($A+B \rightarrow A=B$), (E) full coalescence ($A+B \rightarrow C$), and (F) fragmentation ($A+B \rightarrow n$D).

Figure 1 shows the schematic summary of possible routes for collision between nanocages. A similar classification for the collision of fullerenes has been presented by Campbell *et al.*[5] It is difficult to precisely and strictly characterize the results of fusion. As is shown on Fig. 1, only some the routes lead to fusion between nanoparticles (namely, routes D and E). In case of partial coalescence (case D), only some of the cage bonds are broken, lending a peanut shape to the resulting dimer structure. One can speculate whether the further fusion of peapods to fully coalesced structure (E) is feasible or not. The result of full fullerene coalescence can be either tubulenes (short CNTs) or fullerenes of larger size.[4,5,18] Route B corresponds to fullerene dimerization. This process occurs when the collision energy is not high enough to break more than one or a few bonds. In this case, fullerene adducts rather than coalesced structures are produced. It is sometimes suggested that such dimerization through the formation of a [2+2] (sp^3-joined) cycloadduct is an important initial step in the coalescence of fullerenes.[4,19] For the sake of completeness, we shall also mention "nonreactive" (routes A and C) and fragmentation (panel F) cases. Obviously, the latter results from impacts with collision energies high enough to completely obliterate the cage structures (see also Ref. 5). The case of nonreactive scattering (case A) results from the collision with low impact energy, insufficient to break any cage bond. In the presence of free dangling bonds, such a soft collision could allow the formation of an adduct (case B). For the collision with impact energies large enough to break some of the bonds, the resulting structure may become subject to internal bond reorganization (for example, Stone-Wales-type transformation) without necessarily creating interstructure bonding, hence leading to disconnected cages (route C). This route is denoted as "nonreactive reorganization." This process may be also associated with exchange of atoms between two collision. Nonreactive collisions (case A) and high impact fragmentations (case F) are not within the scope of the present study.

II. COMPUTATIONAL METHODOLOGY

Modeling of collisions was performed by means of direct molecular dynamics based on the SCC-DFTB quantum chemical potential[13–15] in conjunction with Fermi-Dirac smearing at various electronic temperatures to approximately include the effect of electronic excitations[16,17,20] and to improve convergence in the iterative self-consistent-charge scheme. Although all structures consist only of the element carbon and little charge polarization is expected, yet we needed to invoke the self-consistent-charge methodology to prevent unwanted zwitterionic electronic states that can appear in the noncharge-consistent variant of DFTB when a multitude of dangling bonds with similar energies is created. The potential energy for the motions of nuclei is given by the electronic free energy, which is sometimes referred to as Mermin free energy,[21–23]

$$E_{pot} = E_{SCF} - T_{el}S_e. \tag{1}$$

The first term, E_{SCF}, is the electronic energy from the SCC minimization of the electronic structure at a given electronic temperature T_{el}, and the second term, $T_{el}S_e$, describes the electronic entropy contribution associated with the fractional molecular orbital occupancies f_i as follows:

$$S_e = -k_B \sum_{i=1}^{M} [f_i \log(f_i) + (1-f_i)\log(1-f_i)]. \tag{2}$$

The fractional orbital occupancies f_i are determined using a Fermi-Dirac distribution function. We tested the effect of electronic temperature (T_{el}) using the values 0, 1000, 2000, 3000, and 10 000 K. Nuclear motion was followed via classical Newtonian dynamics and velocity Verlet algorithm with time step $dt=1$ fs. No periodic boundary conditions were applied, which means that our collisions are occurring in vacuum.

Prior to collision simulations, we computed a 10 ps thermalization trajectory of a single C_{60} molecule at the temperature $T=1500$ K in order to generate a set of suitable initial structures and velocities for the collision simulations. The Nose-Hoover chain algorithm[24] was used for the initial ther-

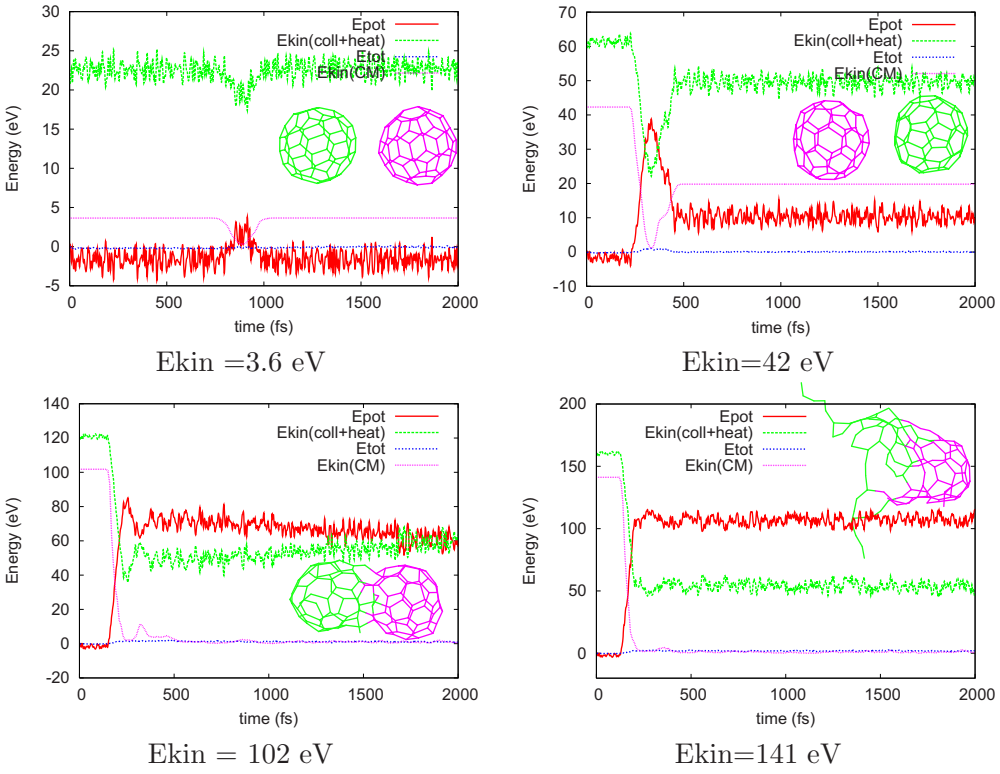

FIG. 2. (Color online) Time dependence of kinetic and potential energy during collision MD between two C_{60} with T_{el}=2000 K. Top left: elastic collision (route A) with CM kinetic energy E_{kin}=3.6 eV. Top right: inelastic collision without significant structure deformation (route A) at E_{kin}=42 eV. Bottom left: collision-induced partial fusion (route D) at E_{kin}=102 eV. Bottom right: collision induced disintegration of carbon skeleton (route F) at E_{kin}=141 eV. The difference between total kinetic energy (green) and collision kinetic energy (purple) is a heat energy (1500 K). At time =0 fs the ordering of plots (from top to bottom) is Ekin(coll+heat), Ekin (CM), Etot (dotted line), Epot (solid line).

malization of C_{60}. The MD simulations of collisions were performed microcanonically and total simulation time equal to 2 ps, starting from randomly selected geometries and velocities from the thermalization run. After the 2 ps collision simulations, we performed long time scale (up to 1 ns) simulations of postcollision relaxation of selected fusion product. The relaxation simulations were performed both microcanonically and canonically with Nose-Hoover chain thermostat and various temperature ramps to model cooling.

The starting structures of C_{60} for collision simulations were selected randomly (both collision partners) from the initial thermalization trajectory. Initial separation (time t=0) between center of mass (CM) of collision partners was set to 20 Å. At such large intermolecular separation there is practically no interaction between C_{60} molecules. Initial structures were randomly rotated to better sample configurational space. The internal vibrational velocities were rotated correspondingly and the incident velocity vector added to the velocities of the projectile C_{60} molecule. We tested the range of incident velocities from 0.6×10^{-3} up to 4.4×10^{-3} a.u. every 0.2×10^{-3} a.u. The corresponding collision kinetic energy with respect to the CM of the combined system was ranging from 3.2 to 172 eV. In comparison, the thermal energy of two C_{60} buckminsterfullerenes at T=1500 K amounts to 23.3 eV.

To include statistical variations, we performed ten independent collision simulations using different starting geometries and velocities from the thermalization trajectory with applied random rotation of the C_{60} orientation for every set of initial conditions (incident velocity, electronic temperature). Overall we performed a total of about 1000 molecular dynamics simulations (20 incident velocities $\times$ 5 values of $T_{el}\times10$ sets of initial structures). All our simulations were restricted to central collision only and we did not consider the effect of rotational dependence in the present study.

III. DISCUSSION OF RESULTS

A. Conservation of energy and the effect of electronic temperature

Figure 2 presents a few examples of total-energy fluctuations with time for MD simulations at T_{el}=2000 K. Overall, the total energy during the simulation is conserved very well and the fluctuation of the total energy (denoted as Etot) are very small (rms smaller than 0.1% of the kinetic energy). For MD trajectories with T_{el}=0 K with the largest incident velocities ($E_{kin}\geq$90 eV), the electronic-structure calculations failed to converge the iterative self-consistent charges. This instability results from the ambiguity of orbital occupations due to the narrowing of the highest occupied molecular orbital (HOMO)/lowest unoccupied molecular orbital (LUMO) gap, which is itself a consequence of the large number of carbon-carbon bonds being broken and then reformed after

TABLE I. Results of collision simulation results for different incident velocities and T_{el} as obtained by visual inspection of trajectories. V_0 is an incident velocity of the C_{60} projectile in $\times 10^{-3}$ a.u. and E_{kin} denotes collisional kinetic energy of both C_{60} units with respect to CM. Table legend: r=bonds reorganization, ex =carbon exchange, op=cage opening, d=dimerization, pF=partial fusion, F=fusion, ev=evaporation of small carbon chains (C_2, C_3, etc.), D=disintegration of fullerenes cage/fragmentation.

No.	V_0	E_{kin}	T_{el}=0 K	1000 K	2000 K	3000 K	10000 K
1	0.6	3.2					
2	0.8	5.4					
…							
11	2.6	59.2					
12	2.8	68.8					d+ex+op
13	3.0	79.1		r+ex		r+ex	r+op
14	3.2	90.0	r+ex	r+ex	r+ex+op		d+ex+op
15	3.4	101.7	d+ex+op	op	pF	r+ex	F
16	3.6	114.1	r+op+ev	pF	r	r+op	F+ev
17	3.8	127.3	pF	F	F	F+ev	F
18	4.0	141.1	F	F	F+ev/D	F	F/D
19	4.2	157.5	F+ev/D	D	D	D	D
20	4.4	172.9	D	D	D	D	D

the high impact collision event. Such a problem is not observed in finite electronic temperature simulations where fractional occupation of orbitals near the Fermi level ensures similar electron occupation for orbitals with similar energies.

In addition to improving the iterative self-consistent-charge algorithm, Fermi-Dirac smearing allows to approximately describe thermal excitation of electrons.[16,17,20] This however brings a question about validity of the SCC-DFTB Hamiltonian to correctly reproduce the excited electronic states. Our recent benchmark simulation of electronic density of states for C_{60} and other fullerenes correctly predict HOMO-LUMO gap and, in agreement with experimental data, suggests that C_{28} is metallic while C_{60} and C_{70} are not.[25] Also, the detailed discussion of electronic excitations with SCC-DFTB Hamiltonian via time-dependent response theory for C_{60} and for polycyclic aromatic hydrocarbons is presented by Niehaus.[26] The SCC-DFTB results in Ref. 26 yields a good agreement for optical spectra with experiments and first-principles calculations. Thus, (a) our recent simulations of electronic density of states benchmark for C_{60} and (b) the discussion presented in Ref. 26 suggest that SCC-DFTB Hamiltonian is a reasonable and computationally inexpensive approach in modeling of low-lying electronic excitations.

A brief summary of trajectories obtained with different electronic temperatures is presented in Table I. Using different values of electronic temperature allow to probe and control in an "average" way the effect of electronic excitation.[20] The results of simulations for different values of electronic temperature are consistent but the trajectories themselves can be different in terms of individual bond breaking and formation events. The overall observed trend is that for the thermally excited electrons the carbon-carbon bonds are weakened as the contribution from excited states increases with T_{el}, and the fusion between fullerenes becomes possible for lower values of the collision energy. This effect complements the thermal activation of nuclei.

B. Time dependence of potential and kinetic energy

Four representative trajectories obtained at T_{el}=2000 K are presented in Fig. 2. The two top panels present nonreactive collision cases, in which both fullerenes bounce back after the collision. The two bottom panels present reactive collision cases, in which extensive carbon bonding reorganization is observed and the entire impact energy is converted into internal energy (heat+potential energy). The time evolution of the total energy is shown in Fig. 2 as E_{tot} (blue line), where we also plot the fluctuation of the total kinetic energy E_{kin}(coll+heat) (green line). The latter consists of two components: (a) translational (collision) kinetic energy and (b) internal vibrations of the carbon cage (heat). The first component, the translational collision kinetic-energy contribution, is denoted as E_{kin}(CM) and is measured with respect to the center of mass of the whole system $C_{60}\ldots C_{60}$ as a sum of translational kinetic energy of CM for each C_{60} subsystem with respect to the CM of total system,

$$E_{kin}(\mathrm{CM}) = E_{kin}(\mathrm{CM}_1) + E_{kin}(\mathrm{CM}_2). \quad (3)$$

The second component, namely, the instantaneous value of the heat, can be obtained as a difference between the total kinetic energy (green), E_{kin}(coll+heat), and the incident kinetic energy E_{kin}(CM). The time of the collision event can be identified from the plot as the sudden drop of E_{kin}(CM). For example, for the cases with E_{kin}(CM) equal to 3.6 and 42 eV the collision occurs at 900 fs and 350 fs, respectively. In these nonreactive cases, both C_{60} units bounce back, and the value of E_{kin}(CM) increases after the collision as both fullerenes start moving apart. The collision kinetic energy E_{kin}(CM) stabilizes at some level once the separation between both fullerene units is large as the interaction between the cages is reduced due to increasing distance. The difference between initial and final E_{kin}(CM) constitutes a fraction the kinetic energy that is (a) converted at the collision into a

heat, and (b) is absorbed into the potential energy by the carbon-bond network deformation induced by the impact.

C. Incident energy dependence of the collision outcome

The collisions with incident kinetic energy smaller than 10 eV can be considered as elastic (route A). The value of E_{kin}(CM) is conserved within ≈1%. The absolute value of the changes in kinetic energy depends on the relative orientation of the colliding partners. Collisions with initial incident energy E_{kin}(CM) larger than 10 eV are inelastic, and we observe a significant transfer of kinetic energy into vibration and carbon-bond deformation E_{pot}. For incident energies between 10 and 60 eV, relatively small deformations of carbon cages (route C) are observed. We do not observe bond breaking in this energy range but only bond stretching and angle deformations. The most interesting (chemically reactive) region is for collisions with incident energies larger than 60 eV, where the impact energy is high enough to allow opening of the carbon cage and significant reorganization of the carbon-bond network.

Table I presents the analysis of collision outcome for various incident energy and electronic temperatures. For incident energy between 60 and 100 eV, the probability for fusion is small. In this energy range, we observed several structural transformations along routes B or C, which do not necessarily lead to fusion. In this energy window, the typical bond transformations include opening of the fullerene cage, internal bond rearrangement/reorganization, evaporation of short carbon chains C_2, C_3, and exchange of carbon atoms between both fullerene units. The fusion of two fullerenes (route D) is dominant in the energy range 100–140 eV. The final kinetic energy E_{kin}(CM) approaches zero after the collision and fusion of both "C_{60}" units. Thus, the entire initial kinetic energy E_{kin}(CM) is transferred into internal heat and potential energy of the carbon-bond network. For the collision energies higher than 140 eV, we mostly observed disintegration of the carbon network and fragmentation (route F). In the first stage of disintegration, the cage and ring structure of fullerenes is destroyed. It develops into an amorphous wirelike bundle, containing carbon chains of various length. This chain structure can relatively easily further break down onto pieces resulting in a total fragmentation of the structure, favored by the gain in entropy at the resulting high temperature and the absence of carbon pressure.

We occasionally observed the collision-induced symmetry change from initially icosahedral structures of both colliding fullerenes to lower symmetry fullerenes after the collision. The example of final structures of C_{60} with symmetry changed from icosahedral to D_{2h} and C_2 as a result of collision is shown in Fig. 3. Within the energy window of 60–100 eV, we also observed dimerization (route B) of fullerenes (see Table I). As can be seen in Table I, in most of the cases the impact effects are combinations of relatively small number of major events, and the structural changes are difficult to characterize quantitatively.

D. Effect of charge and dispersion

The experimental data are available for collisions between neutral C_{60} and ionic C_{60}^+ moieties. However, the current

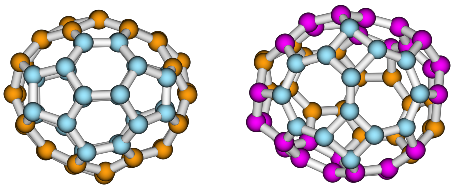

FIG. 3. (Color online) Collision-induced symmetry change for incident kinetic energy equals 79 eV. The initial symmetry of both fullerenes before collision was I_h. The coloring of carbon atoms is chosen to emphasize the symmetry of fullerenes.

Born-Oppenheimer MD simulation scheme is not very suitable for the modeling of collision between neutral and charged fullerenes, as the location of the positive charge is difficult to control during the simulation, leading to unphysical situations when the charge is delocalized on both fullerenes or fluctuates.[23] Delocalization of the charge between colliding partners, in effect, introduces unphysical Coulomb repulsion term to forces between two partially charged $C_{60}^{1/2+}$ species, slowing down the collision process. Nevertheless, we performed simulations of $[C_{60}\ldots C_{60}]^+$ system for selected incident velocities to estimate the effect of positive charge. Our results suggest that for high collision energy, the effect of including charge on the simulation is rather small and can be neglected. Based on (a) the comparison of simulation we performed for neutral and charged systems, and on (b) the fact that large size of fullerenes allows to relatively easily accommodate charge distribution over its structure, and on (c) the very good agreement of our SCC-DFTB simulations with experimental results we do not expect significant differences between collisions of neutral-neutral vs neutral-singly charged species. In our future studies, we will address the question of charge effect and charge transfer in collisions between fullerenes and other species by means of our recently developed Liouville-von Neumann molecular dynamics.[23] In this method, the electronic structures is explicitly (quantum mechanically) propagated in time (subject to initial conditions) rather than minimized as in standard SCF procedure. Thus the dynamical behavior of processes involving electronic charge is described more correctly.

Finally, we also tested the effect of including empirical dispersion term on top of the DFTB energy.[15] We performed simulation with empirical dispersion for a selected incident velocities. Our results suggest that for high collision energy the effect of dispersion forces is insignificant.

E. Comparison with experimental data

A review of experimental data for the collisions between fullerenes and reactions involving fullerenes is presented in Refs. 5 and 27. We repeat here the major findings of this seminal work. The experimental results were obtained for a target C_{60} at an environmental temperature of around 800 K and a projectile temperature of C_{60}^+ equal to 3000 K. (a) The barrier energy for fusion is located somewhere within the 60–80 eV E_{kin}(CM) range[27] (see the left panel of Fig. 4). (b)

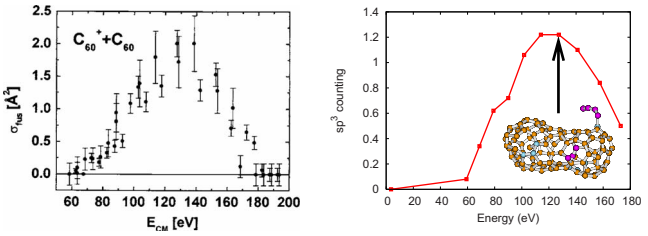

FIG. 4. (Color online) Left: experimental fusion cross section from Ref. 5 for collision between C_{60}^{+} and C_{60}. Right: theoretical average number of sp^3-type carbon atoms from current SCC-DFTB MD collisions between two C_{60} calculated as average over 50 trajectories at any given value of collision energy. Structure beneath is an MD frame from 127.3 eV, T_{el}=2000 K trajectory at time 2 ps (see also Table I). sp-, sp^2-, and sp^3-type carbons are marked by purple, yellow, and cyan, respectively.

The experimental fusion cross section reaches a maximum around 130–140 eV. (c) No fusion products are detected for collision energies higher than approximately 200 eV. Our theoretical findings concerning barrier energy and onset of fragmentation is in very good agreement with experiment, see Table I, considering our observations: (a) we did not observe bond breaking and formation for collision energies lower than 60 eV. (b) At 100 eV, collision energy we observed both molecular fusion and inelastic scattering. The most probable fusion occurs for collision energies around 120–140 eV. (c) For simulation with collision energies around 160 eV and higher the probability of reaction between two fullerenes is high but the overall large amount of available vibration energy in the system leads to postcollision degradation of carbon-bonding structures and increases the probability of fragmentation.

To further compare the results of simulations with the available experimental data we analyzed the occurrence of various types of carbon hybridization[28] for the final structures (after 2 ps of collision simulations). For each set of 50 trajectories at a given value of collision energy, we calculated the average number of sp^n atoms over all 50 final structures (namely, at time 2 ps). We used approximated sp^n counting based on coordination number. Thus, the fourfold-, threefold-, and twofold-coordinated carbon atoms are denoted, respectively, as sp^3, sp^2, and sp^1.[28] We also analyzed the five-, six-, and seven-membered ring counts to detect a chemical signature of fusion reaction. We found that the maximum in the creation of sp^3 atoms is in an excellent agreement with the optimum experimental energy value for the largest fusion cross section (see Fig. 4).

The numbers of all other sp^n carbons (for $n=0,1,2$) are changing monotonically as a function of collision energy ($n=0$ stands for atomic carbon while $n=1$ counts both single- and double-bonded carbon). The number of sp^2-type carbons was decreasing with the collision energy, signaling the disintegration of carbon cage structure of fullerenes. The number of sp^1 carbons was increasing and this indicates the tendency to form linear carbon chains. This suggests that (a) formation of sp^3-type hybridization of carbon is an important intermediate step of a fusion reaction as one might naively expect, (b) the number sp^3 carbons can be used as a convenient indicator of the fusion progress in MD simulations.

Our simulations confirm previously suggested fast redistribution of vibrational energy model.[5] The set of all vibrational degrees of freedom of fullerene cage behaves collectively as an efficient sink for the translational collision energy. The tight, resilient network of carbon-carbon bonding allows fast kinetic-energy transfer away from the spatial impact region and decreases the probability of reaction between fullerenes. In a sense, the high thermal conductivity of the carbon cage provides a bumper mechanism, softening the impact from the collision. This effect is likely to be responsible for very low reactivity and high stability of C_{60} under sudden mechanical stress.

One can expect similar behavior in reactions involving CNTs, where the resilient network and high thermal conductivity of the sp^2 carbon network can efficiently redistribute impact kinetic energy from incoming reactants. Contrary to this, we expect that soft and floppy carbon based nanomolecule in which vibrational modes can be excited locally without significant energy redistribution are much more prone to sudden impact reactions. In consequence, it seems likely that a "static" description of reactions involving impact on fullerenes and CNTs, based purely on a nondynamical analysis of potential energy surface with local changes in a small region of the hypersurface, does not do justice to the dynamic aspects of the problem, and may require inclusion of some model of impact energy redistribution into the static model.

For completeness, one should notice that fullerenes and carbon nanotubes can react and fuse in different from collision situation such as welding of carbon nanotubes under the influence of an electron beam (e.g., in TEM experiments).[29–31] Processes of this kind molecular transformation are on the microseconds and longer time scale which is currently beyond the reach of direct molecular dynamics simulations and thus requires using different theoretical approaches.[3,10]

F. Postcollision relaxation

A notable difference between experimental and theoretical studies is that the experimental detection of fusion products takes place after several hundreds of microsecond[27] whereas such a long time scale is inaccessible for conventional DFT-based MD simulations, which only allow simulations for up to a few picoseconds. Although the critical events leading to fusion or no fusion occur within about 1 ps, the structural relaxation occurs on much longer time scales. In the absence of MD simulations, it was suggested that the relaxation of the peanut structure may lead to more stable cigar-shaped structures, representing a very small CNT.[5,32] Quantum chemical MD simulations based on the SCC-DFTB potential allow to perform simulations up to several hundreds of picoseconds and thus to directly study the relaxation effect. To verify the role of postcollision structural relaxations we performed constant energy (microcanonical) simulations and annealing simulations (to mimic the radiative cooling and effect of secondary collisions).

For the relaxation simulations, we have chosen randomly one of the final structures (and corresponding velocities) at 2

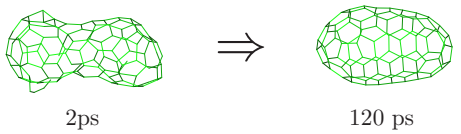

FIG. 5. (Color online) Post collision transformation of a peanut-like structure to a short CNT structure within 200 ps. The collision energy was 127 eV. During relaxation, 20 carbon atoms evaporated from C_{120} fusion product as short chains, leading to the C_{100} structure at 120 ps. Estimated theoretical temperature of two fused fullerenes after collision at 2 ps was 4000 K.

ps time frame from the 127 eV collision trajectories (see left panel in Fig. 5). The estimated temperature of this immediate fusion product calculated as an average over the last 0.5 ps of the collision dynamics is 4000 K (± 2 K). We performed 0.2 ns relaxation simulations both in the microcanonical ensemble as well as by simulated annealing MD with various cooling rates. The simulated annealing runs were performed with the Nose Hoover chain algorithm. The slowest cooling rate applied was 20 K/ps, thus it took 0.2 ns for the longest simulated annealing run to cool down from 4000 to 0 K.

For microcanonical simulations, we observed that the initial peanut-shaped fusion product indeed transforms into short CNT with a cigar shape. 20 carbons evaporated from the initial C_{120} structure in the form of very short carbon chains during the microcanonical relaxation leading to C_{100} final structure (see Figs. 5 and 6). This result is in agreement with Smalley's shrink wrap mechanism and our previously suggested shrinking-hot giant road to fullerenes.[33] The kinetic energy of evaporated carbons was about twice higher (per atom) than those remaining in the fusion product. Our C_{100} structure from the microcanonical relaxation simulations of fusion structure obtained with collision energy 127 eV are very close to the predicted from evaporation model of Klots[34] and are in an excellent agreement with an average atomic mass of C_{60} fusion products observed experimentally (see Fig. 2 in Ref. 27).

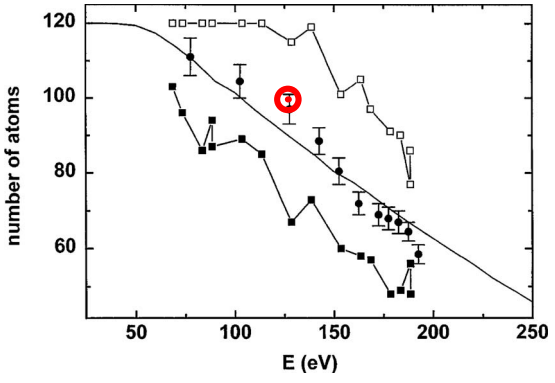

FIG. 6. (Color online) Maximum (open squares), minimum (full squares), and average (full circles) carbon cluster mass observed experimentally as the product of a fusion reaction as a function of collision energy from Ref. 27. The full line is an estimate of the cluster from the statistical thermal evaporation model (Ref. 34). The open circle (red) is result from the current post collision relaxation simulation. For collision energy 127 eV, we observed that 20 carbons evaporated from the hot C_{120} fusion product within 0.2 ns SCC-DFTB dynamics.

To the contrary, we did not observe evaporation of carbons in annealing simulations. In previous constant temperature simulations at 3000 K, we found C_2 evaporation occurring from giant fullerenes once every few hundreds of picoseconds, much slower than the present simulation time. The final structures from simulated annealing simulations was somewhat transformed but remains more or less similar to a peanut rather than to a cigar. Our annealing simulations suggest that the radiative cooling may be in part responsible for the experimentally observed larger masses of fusion product as opposed to low pressure carbon evaporation.

IV. SUMMARY

We performed around 1000 direct hyperthermal collision Born-Oppenheimer MD simulations between two buckminsterfullerenes for initial collision velocities of the projectile C_{60} ranging from 0.6×10^{-3} a.u. (collision energy is 3.2 eV) up to 4×10^{-3} a.u. (collision energy 172 eV), using the quantum chemical SCC-DFTB potential. The simulations were performed for various electronic temperatures and compared with experimental results obtained by Campbell.[5,27] Our theoretical investigation suggests the following: (1) SCC-DFTB provides a convenient, computationally inexpensive, and adequately accurate model for the simulation of high-energy (hyperthermal) collision reactions between nanosized carbon molecules. The effect of including electronic excitation through electronic temperature is small and is comparable to thermal activation of reactants.

(2) Five energy regions can be distinguished in which different collision results dominates: (a) elastic collision region for collision energies smaller than 10 eV, (b) inelastic nonreactive collision with significant heat transfer for collision energies within 10 and 60 eV, (c) inelastic collisions with internal reorganization for energies within 60 and 100 eV, (d) fusion region for collision energies between 100 and 140 eV, (e) disintegration of fullerene cage structure and fragmentation for energies larger than 140 eV.

(3) The crucial, all-determining period of fusion reactions occurs within a relatively short time of about 1 ps. The subsequent relaxation of fusion product occurs on the order of hundreds of picoseconds with evaporation of short carbon chains and transformation of peanut shaped fusion product to structurally more stable short CNT depending on effectiveness of cooling processes/environmental pressure.

(4) The fusion reaction occurs through the formation of sp^3 carbons. The average number of sp^3 carbons from SCC-DFTB simulations is a good indicator of fusion probability and agrees very well with the experimental cross section for fullerene fusion. Important intermediate structures are linear carbon chains that are involved in sp^2 carbon network bond breaking and formation processes.

(5) The presented SCC-DFTB direct MD simulations are in very good agreement with experimental[5,27] findings: (a) energetic fusion window for collision of C_{60} opens at around 60 eV, (b) the probability of fusion reaches maximum at around 120–140 eV and then decreases, (c) the relaxation simulation reproduces very well observations of carbon evaporation, and the predicted atomic mass of around 100

carbon atoms for the fusion product after relaxation is in very good agreement with experimental observations.

(6) Our SCC-DFTB MD simulations do not support static models of fusion reaction in which fusion occurs via cascades of local bond breaking and then reconnections (for example, sequence of [2+2] cyclocadditions followed by SW transformation) as proposed in zipper reaction mechanisms[3] and in Ref. 10. The large number of strongly coupled vibrational modes can efficiently transfer the energy released from local cycloaddition reactions away from the local impact with an incoming reactant. Thus, the resilient carbon cage is an efficient energy sink that prevents local bond breaking.

(7) Besides fusion, several structural transformation can be observed for energies larger than 60 eV. Collision can lead to the change in symmetry, to dimerization, or exchange of carbon atoms between fullerenes.

ACKNOWLEDGMENTS

The present research is supported in part by a grant from AFOSR (Grant No. FA9550-07-1-0395), and by a CREST (Core Research for Evolutional Science and Technology) grant in the Area of High Performance Computing for Multiscale and Multiphysics Phenomena from the Japan Science and Technology Agency (JST). The authors are grateful to PNNL for providing access to high-performance computing resources. S.I. acknowledges support by the Program for Improvement of Research Environment for Young Researchers from Special Coordination Funds for Promoting Science and Technology (SCF) commissioned by MEXT of Japan and by a Grant-in-Aid No. 20550012 from the Japan Society for the Promotion of Sciences (JSPS). J.J. acknowledges support from National Science Foundation (Grant No. ARRA-NSF-EPS-0919436).

*jacek@euch4e.chem.emory.edu
†sirle@iar.nagoya-u.ac.jp
‡morokuma@euch4e.chem.emory.edu

[1] P. Harris, Carbon **45**, 229 (2007).
[2] G. Fleming and M. Ratner, DOE Report 2007 (unpublished); www.sc.doe.gov/bes/reports/abstracts.html#GC
[3] Y. Zhao, B. I. Yakobson, and R. E. Smalley, Phys. Rev. Lett. **88**, 185501 (2002).
[4] C. L. Nagy, M. V. Diudea, and T. S. Balaban, *Reaction Pathways in the Coalescence of Fullerenes* (Nova Science, New York, 2005).
[5] E. E. B. Campbell and F. Rohmund, Rep. Prog. Phys. **63**, 1061 (2000).
[6] C. Yeretzian, K. Hansen, F. Diederich, and R. L. Whetten, Nature (London) **359**, 44 (1992).
[7] E. E. B. Campbell, A. Hielscher, R. Ehlich, V. Schyja, and I. V. Hertel, *Nuclear Physics Concepts in the Study of Atomic Cluster Physics*, Lecture Notes in Physics Vol. 404 (Springer, Berlin, 1992).
[8] E. E. B. Campbell, V. Schyja, R. Ehlich, and I. V. Hertel, Phys. Rev. Lett. **70**, 263 (1993).
[9] T. Guo, P. Nikolaev, A. G. Rinzler, D. Tomanek, D. Colbert, and R. Smalley, J. Phys. Chem. **99**, 10694 (1995).
[10] M. Yoon *et al.*, Phys. Rev. Lett. **92**, 075504 (2004).
[11] C. Jin, K. Suenaga, and S. Iijim, Nat. Nanotechnol. **3**, 17 (2008).
[12] Q. Zhao, F. S. Zhang, and H. Y. Zhou, Sci. China, Ser. G **51**, 765 (2008).
[13] J. C. Slater and G. F. Koster, Phys. Rev. **94**, 1498 (1954).
[14] D. Porezag, T. Frauenheim, T. Köhler, G. Seifert, and R. Kaschner, Phys. Rev. B **51**, 12947 (1995).
[15] M. Elstner, D. Porezag, G. Jungnickel, J. Elsner, M. Haugk, T. Frauenheim, S. Suhai, and G. Seifert, Phys. Rev. B **58**, 7260 (1998).
[16] J. Sokoloff, Ann. Phys. **45**, 186 (1967).
[17] N. D. Mermin, Phys. Rev. **137**, A1441 (1965).
[18] S. Spadoni, L. Colombo, P. Milani, and G. Benedek, Europhys. Lett. **39**, 269 (1997).
[19] M. Rao *et al.*, Science **259**, 955 (1993).
[20] A. Alavi, J. Kohanoff, M. Parrinello, and D. Frenkel, Phys. Rev. Lett. **73**, 2599 (1994).
[21] R. M. Wentzcovitch, J. L. Martins, and P. B. Allen, Phys. Rev. B **45**, 11372 (1992).
[22] M. Weinert and J. W. Davenport, Phys. Rev. B **45**, 13709 (1992).
[23] J. Jakowski and K. Morokuma, J. Chem. Phys. **130**, 224106 (2009).
[24] G. J. Martyna, M. L. Klein, and M. Tuckerman, J. Chem. Phys. **97**, 2635 (1992).
[25] H. A. Witek, S. Irle, G. Zhen, W. A. de Jong, and K. Morokuma, J. Chem. Phys. **125**, 214706 (2006).
[26] T. A. Niehaus, S. Suhai, F. DellaSala, P. Lugli, M. Elstner, G. Seifert, and T. Frauenheim, Phys. Rev. B **63**, 085108 (2001).
[27] F. Rohmund, E. E. B. Campbell, O. Knospe, G. Seifert, and R. Schmidt, Phys. Rev. Lett. **76**, 3289 (1996).
[28] For all carbon atoms of a given structure, we calculated number of other carbons connected to it. We denote isolated carbons as sp^0, carbons with up to two other carbons connected as sp^1, carbons with connectivity equal three as sp^2 while carbons with four other carbons connected as sp^3.
[29] E. Hernández, V. Meunier, B. W. Smith, R. Rurali, H. Terrones, M. Buongiorno Nardelli, M. Terrones, D. E. Luzzi, and J.-C. Charlier, Nano Lett. **3**, 1037 (2003).
[30] M. Terrones, H. Terrones, F. Banhart, J.-C. Charlier, and P. M. Ajayan, Science **288**, 1226 (2000).
[31] D. E. Luzzi and B. W. Smith, Carbon **38**, 1751 (2000).
[32] L. D. Strout, R. L. Murry, C. Xu, W. C. Eckhoff, G. K. Odom, and G. E. Scuseria, Chem. Phys. Lett. **214**, 576 (1993).
[33] S. Irle, G. Zheng, Z. Wang, and K. Morokuma, J. Phys. Chem. B **110**, 14531 (2006).
[34] C. E. Klots, Z. Phys. D: At., Mol. Clusters **20**, 105 (1991).